
Intrinsic properties of the two replicative DNA polymerases of *Pyrococcus abyssi* in replicating abasic sites: possible role in DNA damage tolerance?

Adeline Palud^{1,2}, Giuseppe Villani³, Stéphane L'Haridon², Joël Querellou^{1,2}, Jean-Paul Raffin^{1,2} and Ghislaine Henneke^{1,2,*}

¹ Ifremer, UMR 6197, Laboratoire de Microbiologie des Environnements Extrêmes, BP 70, 29280 Plouzané, France.

² Université de Bretagne Occidentale, UMR 6197, Laboratoire de Microbiologie des Environnements Extrêmes, 29280 Plouzané, France.

³ Institut de Pharmacologie et de Biologie Structurale, CNRS-Université Paul Sabatier Toulouse III, UMR 5089, 205 Route de Narbonne, 31077 Toulouse cedex, France.

*: Corresponding author : G. Henneke, Tel. (+33) 2 98 22 46 09; Fax (+33) 2 98 22 47 57, email address : Ghislaine.Henneke@ifremer.fr

Abstract:

Spontaneous and induced abasic sites in hyperthermophiles DNA have long been suspected to occur at high frequency. Here, *Pyrococcus abyssi* was used as an attractive model to analyse the impact of such lesions onto the maintenance of genome integrity. We demonstrated that endogenous AP sites persist at a slightly higher level in *P. abyssi* genome compared with *Escherichia coli*. Then, the two replicative DNA polymerases, PabpolB and PabpolD, were characterized in presence of DNA containing abasic sites. Both Pabpols had abortive DNA synthesis upon encountering AP sites. Under running start conditions, PabpolB could incorporate in front of the damage and even replicate to the full-length oligonucleotides containing a specific AP site, but only when present at a molar excess. Conversely, bypassing activity of PabpolD was strictly inhibited. The tight regulation of nucleotide incorporation opposite the AP site was assigned to the efficiency of the proof-reading function, because exonuclease-deficient enzymes exhibited effective TLS. Steady-state kinetics reinforced that Pabpols are high-fidelity DNA polymerases onto undamaged DNA. Moreover, Pabpols preferentially inserted dAMP opposite an AP site, albeit inefficiently. While the template sequence of the oligonucleotides did not influence the nucleotide insertion, the DNA topology could impact on the progression of Pabpols. Our results are interpreted in terms of DNA damage tolerance.

42 INTRODUCTION

43 The genome of a living cell continuously undergoes a plethora of both exogenous or
44 endogenous genotoxic attacks. Among the myriad of DNA lesions, the abasic
45 [apurinic/aprimidinic (AP)] sites are one of the most common lesions arising at high steady-
46 state levels, yielding up to 2,000-10,000 lesions per human cell per day by spontaneous
47 hydrolysis of the N-glycosylic bond (Lindahl and Nyberg, 1972; Lindahl, 1993). These lesions
48 can be generated by direct elimination of bases via free radical attacks, as a consequence of cells
49 exposure to chemical and physical agents (Breen and Murphy, 1995; Cadet *et al.*, 1999; Loeb *et*
50 *al.*, 1986). Furthermore, AP sites appear transiently as intermediates of Base Excision Repair
51 (BER) by DNA N-glycosylases (Loeb *et al.*, 1986; Scharer and Jiricny, 2001). Despite the fact
52 that it could be considered as an attractive model, identification and determination of the
53 mutagenic properties of AP sites in hyperthermophilic archaea (HA) remains poorly understood.
54 Presumably, life at high temperature inflicts additional stress to genomic DNA in each cell and
55 very high rates of potentially mutagenic DNA lesions (deamination, depurination, oxidation by
56 hydrolytic mechanisms and subsequent strand breakage) should be expected. However, and
57 interestingly, it was demonstrated that the hyperthermophilic crenarchaeon *Sulfolobus*
58 *Acidocaldarius* exhibits a modest rate of spontaneous mutations nearly close to that of
59 *Escherichia coli* (*E. coli*), raising the question of how HA do to preserve their genome intact in
60 such deleterious environmental conditions (Grogan *et al.*, 2001; Jacobs and Grogan, 1997).
61 To cope with the huge spectrum of impediments that result in genome destabilizing lesions,
62 multiple DNA repair mechanisms have evolved in all organisms to ensure genomic stability
63 (Friedberg *et al.*, 2006; Grogan, 2004; Hoeijmakers, 2001). However, situations can arise in
64 which DNA damage escapes to DNA repair and persists into the genome. Cells have developed

1
2
3 65 DNA damage tolerance mechanisms to tolerate hurdles in DNA either by post-replicative gap
4
5 66 filling, copy-choice DNA synthesis or translesion DNA synthesis (TLS) (Friedberg, 2005;
6
7
8 67 Friedberg *et al.*, 2006). Both bacteria and eukaryotes can tolerate arrested DNA replication by
9
10 68 template switching, therefore avoiding accumulation of mutations (Courcelle *et al.*, 2003;
11
12 69 McGlynn and Lloyd, 2002). Whereas template switching systems remain unknown in archaea,
13
14 70 TLS appears to be conserved within the three kingdoms of life (Boudsocq *et al.*, 2001; Friedberg
15
16 71 *et al.*, 2000; Hubscher *et al.*, 2002; Nohmi, 2006; Pages and Fuchs, 2002; Shimizu *et al.*, 2003;
17
18 72 Yang and Woodgate, 2007). Kinetically, this damage tolerance mechanism can be divided in two
19
20 73 steps: (i) nucleotide insertion opposite the DNA lesion; (ii) extension beyond the lesion.
21
22 74 Depending on the nature of the lesion, the bypass may involve a single or the concerted action of
23
24 75 DNA polymerases (Friedberg, 2005; Friedberg *et al.*, 2005). High-fidelity replicative DNA
25
26 76 polymerases in crenarchaea, bacteria and eukaryotes are intrinsically severely blocked upon
27
28 77 incorporation opposite a lesion such as an abasic site, thus recognizing the illegitimate formed
29
30 78 base pair and entering into futile cycles of insertion/excision (Gruz *et al.*, 2003; Pages *et al.*,
31
32 79 2005; Tanguy Le Gac *et al.*, 2004; Zhao *et al.*, 2004). This phenomenon called 'idling' is
33
34 80 relevant to replicative DNA polymerases harbouring the proofreading 3'-5' exonuclease and
35
36 81 reflects the partitioning of a mispaired DNA template between the exonuclease/polymerase
37
38 82 active sites (Villani *et al.*, 1978). The exonuclease activity acts as a kinetic barrier to TLS by
39
40 83 preventing the stable incorporation of bases opposite the DNA lesion and, therefore, confers the
41
42 84 exquisite accuracy of replicative DNA polymerases to preserve the integrity of the genome
43
44 85 (Khare and Eckert, 2002). In the absence of coding information due to the base loss, most of
45
46 86 replicative DNA polymerases obey to the A-rule, preferentially incorporating a dAMP opposite
47
48 87 the abasic site (Haracska *et al.*, 2001; Lawrence *et al.*, 1990; Shibutani *et al.*, 1997).
49
50
51
52
53
54
55
56
57
58
59
60

1
2
3 88 Conceivably, the DNA sequence context, the structure of the DNA primer lesion and the
4
5 89 replicative DNA polymerase examined can account for the preferential dAMP insertion opposite
6
7
8 90 an abasic site. Currently, the A-rule for replicative DNA polymerases remains under intensive
9
10 91 debates (Hogg *et al.*, 2004; Kroeger *et al.*, 2006; Taylor, 2002).
11
12 92 Here, we used *Pyrococcus abyssi* (*P. abyssi*), as a model for studying the genomic maintenance
13
14 93 at high temperature. This euryarchaeote grows at an optimum of 95°C and is faced to
15
16 94 environmental fluctuations imposed by hydrothermal vents (Erauso *et al.*, 1993; Jolivet *et al.*,
17
18 95 2003). Interestingly, *P. abyssi* is able to duplicate bidirectionally its 1.7 million base-pairs from a
19
20 96 single origin as fast as 45 minutes (Myllykallio *et al.*, 2000) and DNA replication is thought to
21
22 97 be achieved by the two high-fidelity DNA polymerases (*PabpolD* and *PabpolB*) and their
23
24 98 accessory factors (Henneke *et al.*, 2005; Rouillon *et al.*, 2007). Consistent with the existing
25
26 99 translesional systems and the lack of specialised DNA polymerases in *P. abyssi*, we speculate
27
28 100 that one or both *Pabpols* could be involved in damage tolerance. In this study, we determine the
29
30 101 steady-state level of AP sites in *E. coli* and *P. abyssi* at different growth stages. Secondly, we
31
32 102 examine the bypass properties of the exonuclease proficient and deficient replicative *Pabpols*
33
34 103 across an abasic site by varying the DNA topology and sequence context. Finally, steady-state
35
36 104 kinetic was employed to give substantial insights into the role of the proofreading activity of
37
38 105 *Pabpols* for nucleotide incorporation on damaged in comparison with intact DNA templates.
39
40 106 Potential mutagenicity of abasic sites and more generally genomic maintenance in *P. abyssi* are
41
42 107 discussed.
43
44
45
46
47
48
49
50
51
52
53
54
55
56
57
58
59
60

108 **RESULTS**

109 **Rate of endogenous AP sites in *P. abyssi* and *E. coli***

110 Before dissecting the *in vitro* behaviour of the *Pabpols* in the presence of abasic sites, we
111 investigated whether such DNA lesions were present into the genome of *P. abyssi*. The
112 mesophilic bacteria *E. coli* was used as a control. The steady-state level of abasic sites was
113 evaluated during the exponential and stationary phases of growth (Figure 1). In the exponential
114 phase, 2 and 25 abasic sites per 100,000 bp were calculated for *E. coli* and *P. abyssi*, respectively
115 (Figure 1). This value moderately increased to reach the number of 4 and 42 abasic sites per
116 100,000 bp at the stationary phase, for *E. coli* and *P. abyssi*, respectively. Taken together, these
117 data provided evidence for the first time that the genome of the hyperthermophile *P. abyssi* has
118 to deal with the presence of abasic sites. Further, the level of AP sites in *P. abyssi* genome is
119 approximately 10-fold higher than in *E. coli*.

121 **Replication of AP sites containing M13mp18 DNA template by *Pabpols***

122 We first checked the capacity of *Pabpols* to duplicate a circular AP-containing
123 heteropolymeric M13mp18 DNA template. Preparation of this damaged AP-M13mp18 templates
124 is depicted in Figure 2A. Under the conditions employed, 11 apurinic (the predominant lesion)
125 and apyrimidinic sites are introduced per molecules (Schaaper and Loeb, 1981). *Pabpols* were
126 tested in a primer extension assay in the presence of either abasic or undamaged M13mp18
127 templates. DNA elongation of the 5'-end fluorescein labelled oligonucleotide 6 (Table 1) was
128 visualized by product analysis on alkaline agarose gel. In the presence of undamaged DNA
129 template, both *Pabpols* (wild-type or exonuclease-deficient, respectively, *exo+* and *exo-*) could
130 extend the primer but with distinct efficiencies. While *PabpolB* *exo+/exo-* carried out DNA

1
2
3 131 synthesis to the full-length of the unmodified M13mp18 (7,249-nt), *PabpolD* *exo*+/*exo*- did only
4
5 132 extend the primer to 3,600-nt likely due to its sensitivity to secondary structures as already
6
7
8 133 observed (Henneke *et al.*, 2005) (Figure 2B, compare lanes 2 and 4 to 7 and 9). However, when
9
10 134 *PabpolD* *exo*- elongated the undamaged template, a faint band corresponding to the full-length
11
12 135 product was observed (Figure 2B, lane 9), consistent with the lower sensitivity of the *PabpolD*
13
14
15 136 *exo*- to secondary structures. DNA synthesis reactions of the wild-type *Pabpols* with AP
16
17 137 templates gave patterns similar to those obtained with undamaged templates, but with a lower
18
19
20 138 amount of elongated products (Figure 2B, lanes 3 and 8). Therefore, the presence of abasic sites
21
22 139 has an inhibitory effect on *Pabpols* activities. The results obtained with *Pabpols* were compared
23
24 140 to those of T4 DNA polymerase, used as a control. While the relative distribution of the products
25
26
27 141 of DNA replication was different with damaged versus undamaged M13mp18 DNA template,
28
29 142 the lower efficiency of the T4 DNA polymerase (family B) in the presence of DNA lesions was
30
31 143 confirmed (Figure 2B, lanes 12 and 13), as already described (Blanca *et al.*, 2007; Tanguy Le
32
33
34 144 Gac *et al.*, 2004). It should be noted that, when reactions were carried out in the presence of
35
36 145 *Pabpols* *exo*- with damaged DNA, a higher amount of replicated DNA products appeared
37
38 146 (Figure 2B, compare lanes 3 to 5 for *PabpolB* and lanes 8 to 10 for *PabpolD*) indicating that the
39
40 147 proofreading activity of *Pabpols* acts as a kinetic barrier to translesion synthesis onto damaged
41
42
43 148 M13mp18. To further address the inhibitory effect of AP sites onto the DNA polymerising
44
45
46 149 activity of *Pabpols*, quantitative analyses were performed by acid precipitable assay as described
47
48 150 under Experimental procedures. Figure 2 C shows the results of replicating these DNA templates
49
50 151 by *Pabpols*. Both *Pabpols* could discriminate between damaged and intact M13mp18 DNA
51
52 152 template. Indeed, reduced synthetic rates were observed for *Pabpols* independently of the
53
54
55 153 proficient or deficient exonuclease activity, with damaged DNA templates. The presence of AP
56
57
58
59
60

1
2
3 154 sites caused a more pronounced inhibition of replication by *PabpolD*, showing a 183-fold and
4
5 155 55-fold reduction of synthetic rates, respectively, for *PabpolD* *exo*⁺ and *PabpolD* *exo*⁻. In the
6
7
8 156 case of *PabpolB*, a 6-fold and 5-fold reduction of synthetic rates, respectively, for *PabpolB* *exo*⁺
9
10 157 and *PabpolB* *exo*⁻, were caused by AP sites. T4 DNA polymerase (family B), used as a control,
11
12 158 exhibited a reduced replicating activity comparable to that of *PabpolB*. Taken together, these
13
14
15 159 results argued that *Pabpols* discriminate between undamaged or damaged DNA templates, with
16
17 160 distinct reduced polymerising activities, suggesting that the presence of AP sites is rate-limiting.
18
19
20 161

21
22 162 **Replication of AP-containing mini-circular and linear oligonucleotides DNA templates by**
23
24 163 **the wild-type or exonuclease-deficient *PabpolB***

25
26
27 164 Since we provided evidence that DNA synthesis was severely impaired on damaged
28
29 165 M13mp18 for both *Pabpols*, we further investigated the insights of such reduced activities.
30
31 166 Translesional synthesis of a unique AP site from wild-type or exonuclease-deficient *Pabpols*
32
33 167 were examined under running start conditions using either linear or mini-circular
34
35 168 oligonucleotides DNA templates. The presence of the AP site was controlled by using T4 DNA
36
37 169 polymerase as already described (Blanca *et al.*, 2007). While *PabpolB* *exo*⁺ could bypass the
38
39 170 abasic site with moderate efficiency (63%) at a ratio enzyme / DNA of 4:1, under these
40
41 171 conditions *PabpolB* *exo*⁻ displayed almost full translesion synthesis (93%) (Figure 3A, compare
42
43 172 lanes 7 and lanes 14, respectively for *PabpolB* *exo*⁺ and *PabpolB* *exo*⁻). Moreover, *PabpolB*
44
45 173 *exo*⁺ had an increased capacity to stall at the AP site, as showed by the more marked presence of
46
47 174 pausing sites at the lesion (Figure 3A, lanes 3-7). The efficiency of the bypass was dependent on
48
49 175 the amount of the DNA polymerase used and the presence or absence of the 3'- to 5'
50
51 176 exonuclease but, in all cases, a plateau could be reached near the equimolar enzyme / DNA
52
53
54
55
56
57
58
59
60

1
2
3 177 concentrations (Figure 3A, lanes 4-5 and lanes 11-12, respectively for *PabpolB* *exo+* and
4
5 178 *PabpolB* *exo-*). The tolerance of the abasic site was reproducible and confirmed by using a linear
6
7
8 179 73-mer with a different DNA sequence context (data not shown) as already described (Tanguy
9
10 180 Le Gac *et al.*, 2004). When replicating the circular DNA template, the translesion ability of
11
12 181 *PabpolB* *exo+/exo-* was reduced at all enzyme concentrations tested. Interestingly, even at the
13
14 182 highest concentrations of *PabpolB* over the minicircle template, translesion synthesis across the
15
16 183 AP site for *PabpolB* *exo+* only reached 32% at its peak (Figure 3B, lane 7) whereas it was much
17
18 184 more effective, reaching up to 86% for *PabpolB* *exo-* (Figure 3B, lane 13). In addition, under
19
20 185 these saturating conditions, there was a stimulation of strand displacement activity of the two
21
22 186 *PabpolB* versions, as indicated by the proportion of products longer than the 87-mer (Figure 3B,
23
24 187 lane 6-7 and 12-13). Taken together these results indicate that *PabpolB* has the capacity to
25
26 188 replicate past an AP site at high pol/DNA ratio. The proofreading activity of *PabpolB* influences
27
28 189 its translesion capacity and progression of both exonuclease-deficient and proficient *PabpolB* are
29
30 190 reduced in the presence of the mini-circular DNA template.
31
32
33
34
35
36
37
38

39 192 **Replication of AP-containing mini-circular and linear oligonucleotides DNA template by**
40
41 193 **the wild-type or exonuclease-deficient *PabpolD***

42
43 194 The ability of *PabpolD* *exo+/exo-* to bypass an abasic site onto the linear and circular
44
45 195 oligonucleotides DNA templates was analysed and the results are presented in Figure 4. As it can
46
47 196 be seen, *PabpolD* *exo+* could incorporate in front of the AP site but, contrary to *PabpolB*, could
48
49 197 not extend past the lesion both on linear and circular DNA templates at all the enzyme's
50
51 198 concentrations tested (lanes 3-7 in Figure 4A, and in Figure 4B). In addition, accumulation of a
52
53 199 shorter product at position +32 could be detected, indicating the 'idling' activity of the *PabpolD*
54
55
56
57
58
59
60

1
2
3 200 *exo+*. *PabpolD* *exo-* was also blocked at the AP site in the presence of the linear template but
4
5
6 201 longer products past the AP site at position + 34, + 35, and + 36 could be detected, although they
7
8 202 never reached the full-length of the 87-mer, even at saturating enzyme concentrations (Figure
9
10 203 4A, lanes 9-13). Interestingly, 35% of bypass could be measured at a ratio *PabpolD* *exo-* / DNA
11
12 204 of 4:1 on the linear DNA template. Similarly, when the experiments were repeated in the
13
14 205 presence of the minicircle DNA template, a strong block at the AP site (+ 33) could be observed
15
16 206 for *PabpolD* *exo-* present at lower concentration to the DNA template (Figure 4B, lanes 9-10).
17
18 207 Moreover, DNA synthesis continued past the AP site at position + 34, + 35, and + 36, but was
19
20 208 also able to reach up to the full-length 87-mer (Figure 4B, lanes 11-13), when the concentration
21
22 209 of the enzyme was higher than that of the minicircle DNA template. Therefore, in the case of
23
24 210 *PabpolD*, its exonuclease activity prevents translesion synthesis of an abasic site independently
25
26 211 of the structure of DNA template, while the *exo-* mutant shows some bypass capacity that
27
28 212 seems enhanced in the case of a mini-circular DNA.
29
30
31
32
33

34 213

35
36 214 **Steady-state kinetic analysis of nucleotide incorporation of wild-type and exonuclease-**
37
38 215 **deficient *Pabpols* opposite undamaged bases**

39
40 216 *Pabpols* have been designated as replicative DNA polymerases (Henneke *et al.*, 2005).
41
42
43 217 This designation supposes that *Pabpols* must endow with high selectivity for each incoming
44
45 218 nucleotide depending on the nature of the base-containing template. Nucleotide incorporation
46
47 219 kinetics were measured in standing start reactions as described in Experimental procedures.
48
49 220 Incorporation efficiency (k_{cat}/K_m) were measured for the wild-type and exonuclease-deficient
50
51 221 *Pabpols* and the frequency of nucleotide misinsertion was calculated as the ratio of the efficiency
52
53 222 (k_{cat}/K_m) of incorrect nucleotide incorporation to the efficiency (k_{cat}/K_m) of correct nucleotide
54
55
56
57
58
59
60

1
2
3 223 incorporation (Table 2). Both wild-type *Pabpol*s exclusively incorporated the correct dGMP
4
5 224 opposite template C and no misincorporation could be detected. In these conditions, a 5-fold
6
7
8 225 reduced incorporation efficiency for *PabpolD* compared to *PabpolB* was observed as indicated
9
10 226 by the k_{cat}/K_m values. The results obtained with the exonuclease-deficient *Pabpol*s at template C
11
12 227 showed that the correct dGMP was preferentially incorporated but their efficiencies were
13
14 228 dramatically reduced compared to the wild-type enzymes, as judged from the dropped k_{cat}/K_m
15
16 229 values, 55- and 103-fold, respectively, for *PabpolB* and *PabpolD*. In addition, misinsertion
17
18 230 events by the exonuclease-deficient *Pabpol*s at template C were comparable, with preference for
19
20 231 insertion of dTMP > dAMP > dCMP (Table 2). Taken together, these results demonstrate that,
21
22 232 while wild-type *Pabpol*s monitor the instructional base of the template and discriminate between
23
24 233 correct and incorrect nucleotides insertion, exonuclease-deficient *Pabpol*s are much less
25
26 234 efficient.

27
28
29
30
31
32 235
33
34 236 **Steady-state kinetics analysis of nucleotide incorporation of wild-type and exonuclease-**
35
36 237 **deficient *Pabpol*s opposite an AP site**

37
38 238 The efficiency for deoxynucleotide insertion opposite an abasic site for the wild-type
39
40 239 *PabpolB* followed the order dAMP > dTMP and to a lesser extent dGMP. Interestingly, *PabpolB*
41
42 240 *exo +* incorporated a dGMP 8355-fold less efficiently opposite an AP site than opposite the
43
44 241 template C (Table 2). Similarly, as judged by the k_{cat}/K_m values, *PabpolD* *exo +* incorporated
45
46 242 preferentially a dAMP over a dTMP opposite the abasic site with a 20-fold higher magnitude
47
48 243 efficiency. It is noteworthy that the apparent K_m values from the incorporation of nucleotides
49
50 244 opposite the abasic site were always higher than from the insertion of a correct dGMP at
51
52 245 template C. Thus, proficient proofreading *Pabpol*s are sensitive to abasic sites and are not
53
54
55
56
57
58
59
60

1
2
3 246 efficient at inserting a nucleotide opposite such a non-instructive lesion. As observed from the
4
5
6 247 k_{cat}/K_m values, *Pabpol*s exo - inserted a dAMP more efficiently than other deoxynucleotides
7
8 248 opposite the AP site. While incorporation efficiencies of dAMP, dGMP and dTMP were higher
9
10 249 when the proofreading function of *Pabpol*B was deficient, no striking difference was observed
11
12 250 between the wild-type and exonuclease-deficient *Pabpol*D. Therefore, *Pabpol*B and *Pabpol*D
13
14 251 exonuclease-deficient resemble each other in their ability to insert nucleotides opposite an abasic
15
16 252 site with higher efficiencies for dAMP incorporation. Taken together, the data show that, while
17
18 253 wild-type *Pabpol*B does not significantly discriminate among nucleotides for incorporation
19
20 254 opposite an AP site, the exonuclease-deficient *Pabpol*B and both wild-type and exonuclease-
21
22 255 deficient *Pabpol*D were much sensitive to a non-coding lesion that seems to govern the dAMP
23
24
25
26 256 incorporation rather than other dNTPs.
27
28
29
30
31

32 258 **Effect of varying the downstream template base on nucleotide incorporation opposite an** 33 34 259 **AP site by the *Pabpol*s**

35
36 260 The primer-templates used in these experiments were designed in order to examine the
37
38 261 effect of changing the template base (N) at the 5' side of the AP site (X) on the initiation of the
39
40 262 extension of the primer. Nucleotide incorporation was measured in standing start reactions under
41
42 263 standard *Pabpol*s assay conditions. The 32-mer primer (oligonucleotide 6) was annealed to the
43
44 264 four templates differing by the nature of the base N = A, T, G and C at the 5' side of the AP site
45
46 265 (Oligonucleotides 2, 1, 3, 4, respectively) (Figure 5). Extension of the primer in the four
47
48 266 duplexes was conducted in the presence of each of the natural dNTPs. On the one hand, the wild-
49
50 267 type *Pabpol*s exclusively inserted a dAMP opposite the abasic lesion, independently of the
51
52
53 268 sequence context (Figures 5A and 5B). While the percentages of incorporation of a dAMP
54
55
56
57
58
59
60

1
2
3 269 ranged from 46 to 58% for *PabpolD* *exo*⁺, they only reached 18% for *PabpolB* *exo*⁺. The
4
5
6 270 *Pabpols* *exo*⁻ also preferentially incorporated a dAMP opposite the AP site with a higher order of
7
8 271 magnitude compared to the *Pabpols* *exo*⁺. For example, the percentages of incorporation of a
9
10 272 dAMP ranged from 66 to 72% for *PabpolD* *exo*⁻ and 46 to 58% for *PabpolD* *exo*⁺ (Figure 5D
11
12 273 and Figure 5B, respectively). However, unlike *Pabpols* *exo*⁺, the *Pabpols* *exo*⁻ also inserted
13
14 274 other dNMPs opposite the non instructional lesion, following the order:
15
16 275 dAMP>dGMP>dTMP>dCMP for *PabpolB* *exo*⁻ and dAMP>dTMP~dCMP>dGMP for *PabpolD*
17
18 276 *exo*⁻, independently of the sequence context (Figures 5C and 5D, respectively). Thus, these
19
20 277 results demonstrate that nucleotide incorporation opposite an AP site by the *Pabpols* *exo*⁺/*exo*⁻
21
22
23
24 278 is not directed by the nature of the base located at the 5' side of the AP site.
25
26
27
28
29
30
31
32
33
34
35
36
37
38
39
40
41
42
43
44
45
46
47
48
49
50
51
52
53
54
55
56
57
58
59
60

1
2
3 279 **DISCUSSION**
4

5 280 In hyperthermophiles, cellular and environmental stresses encountered by cells are likely
6
7
8 281 to be exacerbated by adaptation to extreme conditions. Cell survival is ensured by a complex
9
10 282 network of DNA events that contributes to the maintenance of the functional integrity of nucleic
11
12 283 acids at high temperature. Here, we have focused the study on *P. abyssi*, an anaerobe
13
14 284 hyperthermophilic euryarchaeota (HA) that thrives at elevated temperature in the immediate
15
16 285 surroundings of deep-sea hydrothermal vents. This is the first report that establishes a
17
18 286 relationship between the specific genomic level of abasic sites and the resulting impact on the
19
20 287 intrinsic properties of replicative DNA polymerases in archaea. These features show that *P.*
21
22 288 *abyssi* can be used as an informative model to analyse the biological relevance of DNA damage
23
24 289 accumulation in the hyperthermophilic chromosome and the underlying genomic maintenance
25
26 290 mechanisms.
27
28
29
30

31 291 The investigation presented here shows that the steady-state level of AP sites into the 1.7
32
33 292 million base-pairs of *P. abyssi* ranged from 25 to 42 AP sites per 100,000 bp during the
34
35 293 exponential and stationary phases, respectively. Similarly, a 2-fold increase of AP sites is
36
37 294 observed in *E. coli*. These findings corroborate the higher efficiency of DNA protection and
38
39 295 repair mechanisms in proliferating cells, compatible with a low level of AP sites. However, it is
40
41 296 important to precise that our expectation to detect a drastic increased number of abasic sites in
42
43 297 the hyperthermophilic chromosome was not fulfilled. Indeed, the level was only 10-fold higher
44
45 298 than in the mesophilic bacteria *E. coli*. Comparatively, the frequency of endogenous AP sites in
46
47 299 mammalian cells reached 10 to 12 AP sites per 100,000 bp (Zhao *et al.*, 2006). Indeed, in the
48
49 300 literature, the number of AP sites in the genome of thermophilic and hyperthermophilic
50
51 301 microorganisms is always suspected to increase drastically compared to the mesophilic
52
53
54
55
56
57
58
59
60

1
2
3 302 counterparts (Grogan, 1998; Grogan, 2000). This assumption takes into account of the intrinsic
4
5 303 properties of the primary structure of DNA at elevated temperatures, corresponding to a 3,000-
6
7 304 fold increase in DNA decay at 100°C (Lindahl, 1993). Conceivably, *P. abyssi* has evolved to
8
9 305 adjust genetically the level of endogenous AP sites in its genome that could be detrimental for
10
11 306 genome integrity of mesophiles. Accumulation of AP sites and, more generally, others DNA
12
13 307 lesions can be envisaged, suggesting that hyperthermophiles are adapted to survive pre-existing
14
15 308 mutations. Clearly, these results establish that the number of AP sites seems to evolve respect to
16
17 309 the growth stage without affecting cell growth and viability. However, further studies are
18
19 310 required to determine the threshold that hyperthermophiles can support to ensure cell survival.
20
21
22
23

24 311 Evolution has produced multiple DNA polymerases able to replicate undamaged or
25
26 312 damaged DNA. Sixteen DNA polymerases have been described in human, nine in
27
28 313 *Saccharomyces cerevisiae*, five in *E. coli* (Bebenek and Kunkel, 2004; Hubscher *et al.*, 2002;
29
30 314 Rothwell and Waksman, 2005) and up to five in archaea (Barry and Bell, 2006; Yang, 2005).
31
32 315 Interestingly, the genome of the euryarchaeota *P. abyssi* encodes only two DNA polymerases,
33
34 316 families B and D, required to faithfully duplicate the genetic information (Henneke *et al.*, 2005).
35
36 317 In this study, steady-state kinetic analyses of nucleotide insertion show for the first time that
37
38 318 *PabpolD* is endowed with high-fidelity onto undamaged DNA as its replicative counterpart,
39
40 319 *PabpolB* (Table 2). Incorporation efficiency of *PabpolD* was reduced to five fold compared to
41
42 320 *PabpolB*, demonstrating that *Pabpols* possesses distinct kinetic properties.
43
44
45
46
47

48 321 Our results give evidence that the presence of AP sites strongly inhibited the DNA polymerising
49
50 322 activity of both *Pabpols* and that the absence of their proofreading function correlate with
51
52 323 enhanced bypass of AP sites. The degree of inhibition of DNA synthesis was dependent upon the
53
54 324 *Pabpol* examined. *PabpolD* could insert a nucleotide opposite the AP site and, in all conditions
55
56
57
58
59
60

1
2
3 325 tested, was not able to extend beyond the 3' primer lesion. *PabpolB* inserted opposite the AP site
4
5 326 and extended the DNA template to the full-length, only when present at a molar excess over the
6
7
8 327 template. This result is comparable to previous studies showing that molar excess of enzyme
9
10 328 versus DNA template could enhance translesion synthesis by DNA polymerases past an abasic
11
12 329 site (Blanca *et al.*, 2007; McCulloch and Kunkel, 2006; Tanguy Le Gac *et al.*, 2004). While
13
14 330 translesion synthesis of both exonuclease-proficient and deficient *PabpolB*s and the exonuclease-
15
16 331 deficient *PabpolD* were differently affected by the topology of the DNA template, the template
17
18 332 sequence context did not significantly influence the bypass properties of *Pabpols*. Further, both
19
20 333 *Pabpols* inserted dAMP opposite the AP site independently of the nature of the 5' template base
21
22 334 to the AP site. Despite this nucleotide selectivity, steady-state kinetics showed that dAMP
23
24 335 incorporation was not efficient. These observations show for the first time that archaeal
25
26 336 replicative (families B and D) DNA polymerases follow the 'A-rule' (Strauss, 1991; Taylor,
27
28 337 2002) like eukaryal and bacterial counterparts (Haracska *et al.*, 2001; Shibutani *et al.*, 1997). The
29
30 338 physical basis of the 'A-rule' is still an intensive debate (Kool, 2002; Zahn *et al.*, 2007) and
31
32 339 structural studies reported the molecular level of replication blockage that produced catalytically
33
34 340 inactive DNA polymerases (Freisinger *et al.*, 2004; Hogg *et al.*, 2004). Whether the molecular
35
36 341 and physical bases are conserved through archaeal replicative DNA polymerases would have to
37
38 342 be unravelled. Accordingly, the ability of abasic sites to inhibit *Pabpols* could reflect steric
39
40 343 constraints imposed by the "tightness" of the active site. Furthermore, the capacity to partition
41
42 344 the mispairs away from the polymerase domain into the exonuclease active site might exhibit
43
44 345 structural rearrangements that are differentially influenced by the dynamic features of the DNA
45
46 346 polymerase. To this point, the major distinction between the two *Pabpols* is the subunits
47
48 347 composition. While *PabpolB* is a monomeric enzyme with associated exonuclease and
49
50
51
52
53
54
55
56
57
58
59
60

1
2
3 348 polymerase activities, *PabpolD* is an heterodimeric enzyme with the large and the small subunits
4
5 349 carrying, respectively, the polymerase and the exonuclease activities (Gueguen *et al.*, 2001).
6
7
8 350 Therefore, it is reasonable to suggest that the architecture of the two DNA polymerases may
9
10 351 account for the subtle differences observed within the polymerase and exonuclease efficiencies.
11
12 352 However, a complete detailed functional analysis must await the crystal structure of the
13
14 353 individual *Pabpols*. The balance between polymerization and excision was recently described in
15
16
17 354 B-family DNA polymerase in archaea (Kuroita *et al.*, 2005) but never in D-family. The distinct
18
19
20 355 kinetic partitioning of insertion and edition of mispairs observed within *Pabpols* corroborates
21
22 356 with eukaryal and bacterial homologues properties (Jin *et al.*, 2003; Jin *et al.*, 2005; Pages *et al.*,
23
24 357 2005) and confers that replicative DNA polymerases are high-fidelity enzymes (Bloom *et al.*,
25
26 358 1997; Chen *et al.*, 2000; Shimizu *et al.*, 2002).
27
28
29 359 The down-regulation of the proofreading function of *PabpolB* could favour TLS in order to
30
31 360 overcome the block imposed by AP sites. Bypass of AP sites could generate either single-base
32
33 361 substitutions or frameshift mutations (Baynton and Fuchs, 2000). *PabpolB* appears to proceed
34
35 362 through single-base substitution upon completion of DNA template containing an AP site. The
36
37
38 363 molar excess of the enzyme over the DNA template accounted for TLS under our *in vitro*
39
40 364 conditions. On the other hand, a replicative *Pabpol* idling at a DNA lesion could be a crucial
41
42 365 factor to trigger cellular responses to DNA damage in *P. abyssi*. The mechanism by which
43
44 366 proofreading activities of archaeal DNA polymerases could be regulated *in vivo* (dNTPs balance,
45
46
47 367 role of accessory proteins and enzymes switching) and their contribution in some cases to
48
49 368 counteract genomic DNA lesions has to be elucidated. Recently, it was described that *P. abyssi*
50
51 369 has evolved with efficient DNA strategies to cope with ionizing radiations and elevated
52
53 370 temperatures (Jolivet *et al.*, 2003). Biochemical evidence for relevant DNA repair mechanisms
54
55
56
57
58
59
60

1
2
3 371 has not been demonstrated in *P. abyssi* yet. More striking is the lack of identification of any
4
5
6 372 mismatch repair genes and the complete set of damage excision genes (Cohen *et al.*, 2003).
7
8 373 Interestingly, homologous recombination genes (RecA/Rad51) have been identified into the
9
10 374 genome sequence of *P. abyssi* together with the fact that exponentially growing thermophilic
11
12 375 archaea contain several copies of the chromosome (Bernander and Poplawski, 1997; Breuert *et*
13
14
15 376 *al.*, 2006). This might be particularly consistent for the repair of strand breaks. Furthermore, it is
16
17 377 not excluded that the recently characterised primase from *P. abyssi* could also play a role in
18
19
20 378 damage avoidance since it possesses sequence and structural similarities with the family X DNA
21
22 379 polymerases (Le Breton *et al.*, 2007). Ultimately, the process of such DNA lesions would have to
23
24 380 be explored by the *P. abyssi* replisome in the context of genomic mutagenicity.
25
26
27
28
29
30
31
32
33
34
35
36
37
38
39
40
41
42
43
44
45
46
47
48
49
50
51
52
53
54
55
56
57
58
59
60

381 **EXPERIMENTAL PROCEDURES**

382 **Strains and cell culture techniques**

383 *P. abyssi* GE5 (Brittany Culture Collection, <http://www.ifremer.fr/souchotheque>) were
384 grown in 50 ml YPS medium under anaerobic conditions at 95°C (Erauso *et al.*, 1993). The *E.*
385 *coli* CIP 54.8 strain (CRBIP) was cultivated in 1 L of Luria-Bertani (LB) broth (1% tryptone,
386 0.5% yeast extract, 1% NaCl) at 37°C and pH 7.3, in a shaking incubator (170 rpm). Growth was
387 monitored by density measurements with a cell Thoma counting chamber (0.02 mm depth).
388 Samples for DNA extraction were collected in the exponential and stationary growth phases as
389 indicated in Figure 1. The samples for DNA extraction were centrifuged at 6,000 g for 15 min at
390 4°C and the pellets were stored at -20°C.

391

392 **Genomic DNA Isolation and Detection of AP sites**

393 Genomic DNA from *P. abyssi* was isolated using the extraction method as described
394 (Charbonnier *et al.*, 1995) and optimised in order to avoid the formation of additional AP sites.
395 Briefly, cell pellets were suspended in 800 µl TE-Na-1 X lysis buffer (100 mM Tris-HCl, 50 mM
396 EDTA, 100 mM NaCl, pH 8.0). This was followed by successive additions of 50 µl proteinase K
397 (20 mg/ml), 100 µl Sarcosyl (10%), 100 µl SDS (10%). The applied lysis treatment were
398 performed at 37°C for 1.5 hours and isolation of the total DNA was accomplished by adding an
399 equal volume of buffered (pH 8.0) PCI (Phenol/Chloroform/Isoamyl Alcohol: 25/24/1). The
400 samples were gently mixed and the aqueous phases were collected by centrifugation at 10,000 g
401 for 10 min at 4°C. 10 µl RNase (10 mg/ml) were added and incubation was performed at 37°C
402 for one hour. DNAs were purified with an equal volume of PCI and centrifuged. The upper phase
403 was extracted with an equal volume of pure chloroform and centrifuged. DNA precipitation was

1
2
3
4
5
6
7
8
9
10
11
12
13
14
15
16
17
18
19
20
21
22
23
24
25
26
27
28
29
30
31
32
33
34
35
36
37
38
39
40
41
42
43
44
45
46
47
48
49
50
51
52
53
54
55
56
57
58
59
60

1
2
3 404 obtained by mixing the final aqueous phase with 0.7 volume of 100% isopropanol followed by
4
5 405 incubation for one hour at room temperature. After a 30 min centrifugation at 15,000 g at 4°C,
6
7 406 the DNA pellets were washed once with 0.5 ml of 70% ice cold ethanol. Finally, the DNA pellets
8
9 407 were air-dried during 1 hour before solubilization in TE-1X buffer (10 mM Tris-HCl, 2 mM
10
11 408 EDTA, pH 7.5).

12
13 409 Genomic DNA extractions from *E. coli* was performed following the CTAB (Hexadecyl
14
15 410 trimethyl-ammonium bromide) method for Gram-negative bacteria as described (Park, 2007).

16
17 411 The level of AP sites in genomic DNA was measured using the DNA damage
18
19 412 quantification –AP site Counting kit from Dojindo Molecular Technologies (Gaithersburg, MD).
20
21 413 DNA pellets were dissolved in TE buffer supplied by the kit and DNA concentrations were
22
23 414 exactly adjusted to 100 ng/μl. Briefly, DNA samples were incubated with the Aldehyde Reactive
24
25 415 Probe (ARP) reagent (N'-aminooxymethylcarbonylhydrazino-D-biotin) that specifically reacted
26
27 416 with the aldehydic ring-opened AP sites (Kow and Dare, 2000; Kubo *et al.*, 1992). The AP sites
28
29 417 tagged with biotin interacted with horseradish peroxidase-streptavidin and AP sites were
30
31 418 colorimetrically detected. For each condition, the average of three measurements per sample was
32
33 419 used in the statistical analyses.

34
35 420

36 37 421 **Chemicals and Enzymes**

38
39 422 Unlabelled dNTPs were from MP Biomedicals. T4 polynucleotide kinase, DNA ligase
40
41 423 and T4 DNA polymerase were from New England Biolabs. *Pabp1D* was cloned, expressed and
42
43 424 purified as described (Henneke *et al.*, 2005). *Pabp1B* (Isis DNA polymerase) and *Pabp1B*
44
45 425 exonuclease-deficient (Pyra DNA polymerase) were purchased from MP Biomedicals. 1 unit of
46
47 426 *Pabp1B* corresponds to the incorporation of 1 nmol of total dTMP into acid-precipitable
48
49
50
51
52
53
54
55
56
57
58
59
60

1
2
3 427 material per min at 65°C in a standard assay containing 0.5 µg (nucleotides) of
4
5 428 poly(dA)/oligo(dT)_{10:1}. All other reagents were of analytical grade and purchased from Sigma-
6
7 429 Aldrich and Fluka.
8
9

10 430

11
12
13 431 **Construction, expression and purification of the recombinant wild-type and exonuclease-**
14
15 432 **deficient His tag *PabpolD***

16
17 433 The pET26b expression vector containing the *PabpolD* large subunit (DP2) (Gueguen *et*
18 434 *al.*, 2001) was digested with *NdeI* and *SalI* and the resulting fragment was inserted into the
19
20 435 pET28a expression vector (Novagen) in order to introduce a histidine tag (His tag) at the N-
21
22 436 terminus. To render the *PabpolD* exonuclease-deficient, site-directed mutagenesis was carried
23
24 437 out by introducing the H451A point mutation onto the *PabpolD* small subunit (DP1) (Gueguen *et*
25
26 438 *al.*, 2001). The two site-specific complementary primers, reverse H451A 5'-
27
28 439 TGGCCTAGCGGCATCGGCATTTCTGGCCCTAT-3' and forward H451A 5'-
29
30 440 ATAGGGCCAGGAAATGCCGATGCCGCTAGGCCA-3' were used to PCR amplify the
31
32 441 pARHS expression vector containing DP1 according to the protocol of the Quick change
33
34 442 Mutagenesis kit (Stratagene, La Jolla, CA). DNA sequencing was used to confirm that no
35
36 443 spurious mutations had been introduced during PCR. The constructed expression vectors
37
38 444 pET28a/DP2 and either the wild-type or the exonuclease-deficient pARHS/DP1 were co-
39
40 445 introduced into host *E. coli* HMS174 (DE3). The transformed cells were grown in 1.5 liters Luria
41
42 446 Bertani (LB) medium containing ampicillin (100 µg/ml) and kanamycin (30 µg/ml) at 37 °C.
43
44 447 When A_{600} reached 0.7, 1 mM isopropylthio-β-D-galactoside was added to induce expression of
45
46 448 active DNA polymerases. After being cultured 4 hours at 37 °C with gentle shaking (160 rpm),
47
48 449 the cells were harvested by centrifugation, resuspended in 25 ml buffer A (20 mM sodium
49
50
51
52
53
54
55
56
57
58
59
60

1
2
3 450 phosphate, pH 6.6, 1 mM DTT, 20 mM Imidazole) containing the protease inhibitor, disrupted
4
5
6 451 on ice by French press and then heat-treated at 80°C for 15 min. Denatured host proteins were
7
8 452 removed by centrifugation. The clarified supernatant was applied further onto Ni²⁺-HisTrap
9
10 453 column (5 ml of bed volume) pre-equilibrated with buffer A. Proteins were eluted with buffer B
11
12 454 (20 mM sodium phosphate, pH 6.6, 1 mM DTT, 500 mM Imidazole and active fractions were
13
14
15 455 pooled and dialysed against buffer C (20 mM sodium phosphate, pH 6.6, 1 mM DTT). The
16
17 456 dialysate was loaded onto a heparin column (5 ml of bed volume) pre-equilibrated with buffer D
18
19
20 457 (20 mM sodium phosphate, pH 6.6, 1 mM DTT, 0.15 M NaCl). The column was developed with
21
22 458 a linear gradient from buffer D to buffer E (20 mM sodium phosphate, pH 6.6, 1 mM DTT, 1 M
23
24 459 NaCl). Eluted protein showed over 98% purity. Pure His-*Pab*polD (wild-type and exonuclease-
25
26 460 deficient) were dialyzed against storage buffer (25 mM Tris-HCl, pH 8.0, 1 mM DTT, and 50%
27
28 461 glycerol) and stored at -20 °C until use. We checked by acid precipitable assay, as described
29
30 462 (Henneke *et al.*, 2005), that the addition of the His tag at the N terminus of DP2 had no effect on
31
32 463 the DNA polymerization activities. Moreover, the 3'-5' exonuclease deficiency for the mutant
33
34 464 H451A was confirmed (data not shown). Sequence alignment of exonuclease domain in
35
36 465 representative euryarchaeal DNA polymerases highlighting residues critical for proofreading
37
38 466 function is shown in Figure S1.
39
40
41
42
43
44
45

468 **Nucleic Acid Substrates**

469 Single-stranded (ss) M13mp18 was purchased (Amersham Biosciences, GE Healthcare).
470 In order to create AP sites into natural DNA templates, the ssM13mp18 viral DNA was
471 incubated at a final concentration of 0.18 pmol/μl in 30 mM potassium chloride, 10 mM sodium
472 citrate, pH 3.0 at 70°C for 45 min (Schaaper *et al.*, 1983). These conditions introduced one AP
473
474
475
476
477
478
479
480

1
2
3 473 sites per molecule in 4 min, measured by survival (Schaaper and Loeb, 1981). After treatment,
4
5
6 474 the damaged M13mp18 was purified with the QIAquick® PCR Purification Kit from Qiagen
7
8 475 (Germany).
9

10
11 476 The sequences of the DNA primers / templates used in the present study are depicted in
12
13 477 Table 1. All oligonucleotides, including those containing a tetrahydrofuran moiety mimicking an
14
15 478 abasic site, were chemically synthesized and gel-purified (Eurogentec, Belgium). Primers were
16
17 479 labelled at their 5'-end by fluorescein with the 5' End Tag kit labelling system from Vector
18
19
20 480 Laboratories (California). Free fluorescein was removed through the Microspin G-25 column
21
22 481 (Amersham Biosciences, GE Healthcare) and the labelled primers were hybridised to the
23
24
25 482 respective templates at equimolar concentrations.
26

27 483 The minicircle template was prepared as described (Tanguy Le Gac *et al.*, 2004). Briefly,
28
29 484 the linear 5'-phosphorylated oligonucleotide 1 (intact or containing the tetrahydrofuran moiety)
30
31
32 485 was intramolecularly ligated under dilute conditions using a scaffold 40-mer oligonucleotide (5'-
33
34 486 ATATTCCTACCCTCCCGATCTATCCACCATACTACCCTCC- 3'). Minicircles were gel-
35
36
37 487 purified and their concentration was determined spectrophotometrically, followed by annealing
38
39 488 with their complementary 5'-fluorescein labelled primer at equimolar concentration.
40

41 489

42 43 44 490 **Primer extension onto intact or damaged primed-oligonucleotides**

45
46 491 "Standing start" and "Running start" assays were catalysed into a final volume (15 µl)
47
48 492 containing the following components: (i) for *PabpolD*: 8.3 nM of labelled primers / templates, 20
49
50 493 nM of *PabpolD* *exo*+/*exo*- unless otherwise specified, 10 mM Tris-HCl (pH 9.0), 50 mM KCl,
51
52 494 10 mM MgCl₂ and 200 µM dNTPs; (ii) for *PabpolB*: 8.3 nM of labelled primers / templates, 13
53
54
55 495 nM of *PabpolB* *exo*+/*exo*- unless otherwise mentioned, 50 mM Tris-HCl (pH 8.8), 50 mM KCl,
56
57
58
59
60

1
2
3 496 1 mM DTT, 2 mM MgCl₂ and 200 μM dNTPs. Reactions were performed at 55°C for 30
4
5
6 497 minutes and quenched by the addition of 15 μl of stop buffer (98% formamide, 10 mM EDTA).
7
8 498 Samples were heated at 95°C for 5 minutes. The reactions products were resolved on 15%
9
10 499 polyacrylamide, 7 M urea gels and visualized with a Mode Imager Typhoon 9400 (Amersham
11
12 500 Biosciences, GE Healthcare). Quantification of the results was performed using ImageQuant 5.2
13
14
15 501 software. The extent of the bypass reaction was calculated as the ratio of the intensity of the
16
17 502 bands downstream of the AP site to the intensity of the bands opposite the lesion.

19
20 503 Effect of sequence context on AP site bypass was analysed under standing start
21
22 504 conditions. The fluorescein-labelled primer (oligonucleotide 6) was annealed right before the
23
24 505 template AP site that is indicated by X. Different template bases 5' to the AP site are depicted by
25
26
27 506 N (N=A, oligonucleotide 2; N=T, oligonucleotide 1; N=G, oligonucleotide 3; N=C,
28
29 507 oligonucleotide 4) (Table 1). Bypass assays were performed as described above excepted that 16
30
31 508 nM of DNA templates were used when the template base 5' to the AP site was: N=T and N=C
32
33
34 509 for *PabpolB* exo-, N=T and N=G for *PabpolD* exo+, N=C for *PabpolB* exo+. Quantification of
35
36 510 nucleotides insertion opposite the AP site are calculated for wild-type and exonuclease-deficient
37
38 511 *Pabpol*s in triplicate but only the more resolving gel was quantified.

40
41 512

42 43 513 **Steady-state Kinetic Analyses**

44
45
46 514 A 5'-fluorescein labelled primer, annealed to either a correct or damaged template, was
47
48 515 extended in the presence of increasing concentrations of a single dNTP. *Pabpol*s concentrations
49
50 516 and reaction times were set so that maximal product formation was \leq 20% of the substrate
51
52
53 517 concentration. The linear primer-template (oligonucleotides 6 and 1) was extended with dNTP at
54
55 518 55°C in the presence of 6.6-33.3 nM enzyme for 1 or 5 min, depending on the proper utilization
56
57
58
59
60

1
2
3 519 efficiency and substrate utilisation. All reactions (15 μ l) were carried out at various dNTP
4
5 520 concentrations (in triplicate) and quenched with 2 volumes of a solution of 20 mM EDTA in 95%
6
7 521 formamide (v/v). Products were resolved using a 15% polyacrylamide (w/v) electrophoresis gel
8
9 522 containing 7 M urea and visualized using a Mode Imager Typhoon 9400. Bands were quantified
10
11 523 with ImageQuant 5.2 software (Amersham Biosciences, GE Healthcare). The observed rates of
12
13 524 deoxynucleotide incorporation as a function of dNTP concentration were firstly determined from
14
15 525 Lineweaver-Burk plots. The data were fit by nonlinear regression using the Marquardt-
16
17 526 Levenberg algorithm (EnzFitter 2.0, BioSoft) to the Michaelis-Menten equation describing a
18
19 527 hyperbola, $v = (V_{max} \times [dNTP]/K_m + [dNTP])$ as already described (Le Breton *et al.*, 2007).
20
21 528 Apparent K_m and V_{max} kinetic parameters were obtained from the fit and were used to calculate
22
23 529 the efficiency of deoxynucleotide incorporation (k_{cat}/K_m). The kinetics values are the average of
24
25 530 at least triplicate determinations and are shown with standard deviations (SD). ND, means that
26
27 531 no detectable incorporation was observed. Gel patterns and quantitation of single nucleotide
28
29 532 incorporation reactions are shown in Figure S2.
30
31
32
33
34
35
36
37
38

39 534 **Primer extension onto intact or damaged M13mp18 DNA template**

40
41
42 535 *Product analysis.* The oligonucleotide 6 was annealed to either the damaged AP-
43
44 536 M13mp18 or undamaged M13mp18 at a molar ratio 3:1. Standard *Pabpols* reactions (10 μ l) were
45
46 537 conducted into their respective buffer containing 200 μ M each of dNTPs, 7 nM of DNA template
47
48 538 and 2 pmol of *Pabpols*. Reactions were carried out at 60°C for 30 minutes. T4 DNA polymerase
49
50 539 reactions were performed at 37°C for 30 minutes into the 1 X T4 pol buffer (according to the
51
52 540 manufacturer's protocol) with 7 nM of DNA template, 100 μ M each of dNTPs and 2 pmol of T4
53
54
55 541 DNA polymerase. Reaction mixtures were stopped by the addition of 10 μ l of 30 mM EDTA and
56
57
58
59
60

1
2
3 542 the samples were heated to 100°C for 10 min. Reactions mixtures were subjected to a 0.8% (w/v)
4
5 543 denaturing alkaline agarose gel electrophoresis, and replication products were visualized with a
6
7 544 Mode Imager Typhoon 9400 (Amersham Biosciences, GE Healthcare). DNA ladders (Raoul
8
9 545 markers, MP Biomedicals) were run into the same gel and revealed separately.
10
11
12

13 546 *Acid precipitable assay.* The reaction buffers composition were identical to those
14
15 547 described in product analysis for *Pabpols* and T4 DNA pol. The final volume of 10 µl contained
16
17 548 200 µM of unlabeled dNTPs, 20 µM [³H]dTTP, 7 nM of DNA template (AP-M13mp18 or
18
19 549 undamaged M13mp18) and 2 pmol of enzyme to be tested. Reactions were carried out at 60°C
20
21 550 and 37°C, respectively, for *Pabpols* and T4 DNA pol for 30 minutes. DNA was precipitated with
22
23 551 10% trichloroacetic acid (TCA). Insoluble radioactive material was determined by scintillation
24
25 552 counting as described (Henneke *et al.*, 2005; Rouillon *et al.*, 2007).
26
27
28
29
30
31
32
33
34
35
36
37
38
39
40
41
42
43
44
45
46
47
48
49
50
51
52
53
54
55
56
57
58
59
60

1
2
3 553 **ACKNOWLEDGEMENTS**
4

5
6 554 We especially thank Kihei Kubo (Osaka Prefecture University, Sakai, Japan) for helpful
7
8 555 technical comments on the Dojindo Kit. In addition, we thank Robert Fuchs for critical reading
9
10 556 of the manuscript and very helpful discussions. This work was supported by IFREMER and the
11
12
13 557 Région Bretagne. G.V. was supported by CNRS and ARC (grant 4969).
14
15
16
17
18
19
20
21
22
23
24
25
26
27
28
29
30
31
32
33
34
35
36
37
38
39
40
41
42
43
44
45
46
47
48
49
50
51
52
53
54
55
56
57
58
59
60

For Peer Review

1
2
3 558 **REFERENCES**
4

- 5
6 559 Barry, E.R., and Bell, S.D. (2006) DNA replication in the archaea. *Microbiol Mol Biol Rev* **70**:
7
8 560 876-887.
9
- 10 561 Baynton, K., and Fuchs, R.P. (2000) Lesions in DNA: hurdles for polymerases. *Trends Biochem*
11
12 562 *Sci* **25**: 74-79.
13
- 14
15 563 Bebenek, K., and Kunkel, T.A. (2004) Functions of DNA polymerases. *Adv Protein Chem* **69**:
16
17 564 137-165.
18
- 19
20 565 Bernander, R., and Poplawski, A. (1997) Cell cycle characteristics of thermophilic archaea. *J*
21
22 566 *Bacteriol* **179**: 4963-4969.
23
- 24
25 567 Blanca, G., Delagoutte, E., Tanguy le Gac, N., Johnson, N.P., Baldacci, G., and Villani, G.
26
27 568 (2007) Accessory proteins assist exonuclease-deficient bacteriophage T4 DNA
28
29 569 polymerase in replicating past an abasic site. *Biochem J* **402**: 321-329.
30
- 31
32 570 Bloom, L.B., Chen, X., Fygenon, D.K., Turner, J., O'Donnell, M., and Goodman, M.F. (1997)
33
34 571 Fidelity of Escherichia coli DNA polymerase III holoenzyme. The effects of beta, gamma
35
36 572 complex processivity proteins and epsilon proofreading exonuclease on nucleotide
37
38 573 misincorporation efficiencies. *J Biol Chem* **272**: 27919-27930.
39
- 40
41 574 Boudsocq, F., Iwai, S., Hanaoka, F., and Woodgate, R. (2001) Sulfolobus solfataricus P2 DNA
42
43 575 polymerase IV (Dpo4): an archaeal DinB-like DNA polymerase with lesion-bypass
44
45 576 properties akin to eukaryotic poleta. *Nucleic Acids Res* **29**: 4607-4616.
46
47
- 48
49 577 Breen, A.P., and Murphy, J.A. (1995) Reactions of oxyl radicals with DNA. *Free Radic Biol*
50
51 578 *Med* **18**: 1033-1077.
52
- 53
54 579 Breuert, S., Allers, T., Spohn, G., and Soppa, J. (2006) Regulated polyploidy in halophilic
55
56 580 archaea. *PLoS ONE* **1**: e92.
57
58
59
60

- 1
2
3 581 Cadet, J., Delatour, T., Douki, T., Gasparutto, D., Pouget, J.P., Ravanat, J.L., and Sauvaigo, S.
4
5 582 (1999) Hydroxyl radicals and DNA base damage. *Mutat Res* **424**: 9-21.
6
7
8 583 Charbonnier, F., Forterre, P., Erauso, G., and Prieur, D. (1995) Purification of Plasmids from
9
10 584 Thermophilic and Hyperthermophilic Archaea. In *Archaea: A Laboratory Manual*. F.T.
11
12 585 Robb, A.R.P. (ed): Cold Spring Harbor Laboratory Press, pp. 87-90.
13
14
15 586 Chen, X., Zuo, S., Kelman, Z., O'Donnell, M., Hurwitz, J., and Goodman, M.F. (2000) Fidelity
16
17 587 of eucaryotic DNA polymerase delta holoenzyme from *Schizosaccharomyces pombe*. *J*
18
19 588 *Biol Chem* **275**: 17677-17682.
20
21
22 589 Cohen, G.N., Barbe, V., Flament, D., Galperin, M., Heilig, R., Lecompte, O., Poch, O., Prieur,
23
24 590 D., Querellou, J., Ripp, R., Thierry, J.C., Van der Oost, J., Weissenbach, J., Zivanovic,
25
26 591 Y., and Forterre, P. (2003) An integrated analysis of the genome of the hyperthermophilic
27
28 592 archaeon *Pyrococcus abyssi*. *Mol Microbiol* **47**: 1495-1512.
29
30
31 593 Courcelle, J., Donaldson, J.R., Chow, K.H., and Courcelle, C.T. (2003) DNA damage-induced
32
33 594 replication fork regression and processing in *Escherichia coli*. *Science* **299**: 1064-1067.
34
35
36 595 Erauso, G., Reysenbach, A.L., Godfroy, A., Meunier, J.R., Crump, B., Partensky, F., Baross,
37
38 596 J.A., Marteinson, V., Barbier, G., Pace, N.R., and Prieur, D. (1993) *Pyrococcus abyssi*
39
40 597 sp. nov., a new hyperthermophilic archaeon isolated from a deep-sea hydrothermal vent.
41
42 598 *Archives of Microbiology* **160**: 338-349.
43
44
45 599 Freisinger, E., Grollman, A.P., Miller, H., and Kisker, C. (2004) Lesion (in)tolerance reveals
46
47 600 insights into DNA replication fidelity. *Embo J* **23**: 1494-1505.
48
49
50 601 Friedberg, E.C., Feaver, W.J., and Gerlach, V.L. (2000) The many faces of DNA polymerases:
51
52 602 strategies for mutagenesis and for mutational avoidance. *Proc Natl Acad Sci U S A* **97**:
53
54 603 5681-5683.
55
56
57
58
59
60

- 1
2
3 604 Friedberg, E.C. (2005) Suffering in silence: the tolerance of DNA damage. *Nat Rev Mol Cell*
4
5 605 *Biol* **6**: 943-953.
6
7
8 606 Friedberg, E.C., Lehmann, A.R., and Fuchs, R.P. (2005) Trading places: how do DNA
9
10 607 polymerases switch during translesion DNA synthesis? *Mol Cell* **18**: 499-505.
11
12
13 608 Friedberg, E.C., Walker, G.C., Siede, W., Wood, R.D., Schultz, R.A., and Ellenberger, T. (2006)
14
15 609 Biological Responses to DNA Damage. In *DNA Repair and Mutagenesis*. Press, A. (ed).
16
17 610 Washington, D.C., pp. 3-7.
18
19
20 611 Grogan, D.W. (1998) Hyperthermophiles and the problem of DNA instability. *Molecular*
21
22 612 *Microbiology* **28**: 1043-1049.
23
24
25 613 Grogan, D.W. (2000) The question of DNA repair in hyperthermophilic archaea. *Trends*
26
27 614 *Microbiol* **8**: 180-185.
28
29
30 615 Grogan, D.W., Carver, G.T., and Drake, J.W. (2001) Genetic fidelity under harsh conditions:
31
32 616 analysis of spontaneous mutation in the thermoacidophilic archaeon *Sulfolobus*
33
34 617 *acidocaldarius*. *Proc Natl Acad Sci U S A* **98**: 7928-7933.
35
36
37 618 Grogan, D.W. (2004) Stability and repair of DNA in hyperthermophilic Archaea. *Curr Issues*
38
39 619 *Mol Biol* **6**: 137-144.
40
41
42 620 Gruz, P., Shimizu, M., Pisani, F.M., De Felice, M., Kanke, Y., and Nohmi, T. (2003) Processing
43
44 621 of DNA lesions by archaeal DNA polymerases from *Sulfolobus solfataricus*. *Nucleic*
45
46 622 *Acids Res* **31**: 4024-4030.
47
48
49 623 Gueguen, Y., Rolland, J.L., Lecompte, O., Azam, P., Le Romancer, G., Flament, D., Raffin, J.P.,
50
51 624 and Dietrich, J. (2001) Characterization of two DNA polymerases from the
52
53 625 hyperthermophilic euryarchaeon *Pyrococcus abyssi*. *Eur J Biochem* **268**: 5961-5969.
54
55
56
57
58
59
60

- 1
2
3 626 Haracska, L., Unk, I., Johnson, R.E., Johansson, E., Burgers, P.M., Prakash, S., and Prakash, L.
4
5
6 627 (2001) Roles of yeast DNA polymerases delta and zeta and of Rev1 in the bypass of
7
8 628 abasic sites. *Genes Dev* **15**: 945-954.
9
10 629 Henneke, G., Flament, D., Hubscher, U., Querellou, J., and Raffin, J.P. (2005) The
11
12 630 hyperthermophilic euryarchaeota *Pyrococcus abyssi* likely requires the two DNA
13
14 631 polymerases D and B for DNA replication. *J Mol Biol* **350**: 53-64.
15
16
17 632 Hoeijmakers, J.H. (2001) Genome maintenance mechanisms for preventing cancer. *Nature* **411**:
18
19 633 366-374.
20
21
22 634 Hogg, M., Wallace, S.S., and Doublet, S. (2004) Crystallographic snapshots of a replicative
23
24 635 DNA polymerase encountering an abasic site. *Embo J* **23**: 1483-1493.
25
26
27 636 Hubscher, U., Maga, G., and Spadari, S. (2002) Eukaryotic DNA polymerases. *Annu Rev*
28
29 637 *Biochem* **71**: 133-163.
30
31
32 638 Jacobs, K.L., and Grogan, D.W. (1997) Rates of spontaneous mutation in an archaeon from
33
34 639 geothermal environments. *J Bacteriol* **179**: 3298-3303.
35
36
37 640 Jin, Y.H., Ayyagari, R., Resnick, M.A., Gordenin, D.A., and Burgers, P.M. (2003) Okazaki
38
39 641 fragment maturation in yeast. II. Cooperation between the polymerase and 3'-5'-
40
41 642 exonuclease activities of Pol delta in the creation of a ligatable nick. *J Biol Chem* **278**:
42
43 643 1626-1633.
44
45
46 644 Jin, Y.H., Garg, P., Stith, C.M., Al-Refai, H., Sterling, J.F., Murray, L.J., Kunkel, T.A., Resnick,
47
48 645 M.A., Burgers, P.M., and Gordenin, D.A. (2005) The multiple biological roles of the 3'-
49
50 646 >5' exonuclease of *Saccharomyces cerevisiae* DNA polymerase delta require switching
51
52
53 647 between the polymerase and exonuclease domains. *Mol Cell Biol* **25**: 461-471.
54
55
56
57
58
59
60

- 1
2
3 648 Jolivet, E., Matsunaga, F., Ishino, Y., Forterre, P., Prieur, D., and Myllykallio, H. (2003)
4
5 649 Physiological responses of the hyperthermophilic archaeon "Pyrococcus abyssi" to DNA
6
7 650 damage caused by ionizing radiation. *J Bacteriol* **185**: 3958-3961.
8
9
10 651 Khare, V., and Eckert, K.A. (2002) The proofreading 3'→5' exonuclease activity of DNA
11
12 652 polymerases: a kinetic barrier to translesion DNA synthesis. *Mutat Res* **510**: 45-54.
13
14
15 653 Kool, E.T. (2002) Active site tightness and substrate fit in DNA replication. *Annu Rev Biochem*
16
17 654 **71**: 191-219.
18
19
20 655 Kow, Y.W., and Dare, A. (2000) Detection of abasic sites and oxidative DNA base damage
21
22 656 using an ELISA-like assay. *Methods* **22**: 164-169.
23
24
25 657 Kroeger, K.M., Kim, J., Goodman, M.F., and Greenberg, M.M. (2006) Replication of an
26
27 658 oxidized abasic site in Escherichia coli by a dNTP-stabilized misalignment mechanism
28
29 659 that reads upstream and downstream nucleotides. *Biochemistry* **45**: 5048-5056.
30
31
32 660 Kubo, K., Ide, H., Wallace, S.S., and Kow, Y.W. (1992) A novel, sensitive, and specific assay
33
34 661 for abasic sites, the most commonly produced DNA lesion. *Biochemistry* **31**: 3703-3708.
35
36
37 662 Kuroita, T., Matsumura, H., Yokota, N., Kitabayashi, M., Hashimoto, H., Inoue, T., Imanaka, T.,
38
39 663 and Kai, Y. (2005) Structural mechanism for coordination of proofreading and
40
41 664 polymerase activities in archaeal DNA polymerases. *J Mol Biol* **351**: 291-298.
42
43
44 665 Lawrence, C.W., Borden, A., Banerjee, S.K., and LeClerc, J.E. (1990) Mutation frequency and
45
46 666 spectrum resulting from a single abasic site in a single-stranded vector. *Nucleic Acids Res*
47
48 667 **18**: 2153-2157.
49
50
51 668 Le Breton, M., Henneke, G., Norais, C., Flament, D., Myllykallio, H., Querellou, J., and Raffin,
52
53 669 J.P. (2007) The heterodimeric primase from the euryarchaeon Pyrococcus abyssi: a
54
55 670 multifunctional enzyme for initiation and repair? *J Mol Biol* **374**: 1172-1185.
56
57
58
59
60

- 1
2
3 671 Lindahl, T., and Nyberg, B. (1972) Rate of depurination of native deoxyribonucleic acid.
4
5 672 *Biochemistry* **11**: 3610-3618.
6
7
8 673 Lindahl, T. (1993) Instability and decay of the primary structure of DNA. *Nature* **362**: 709-715.
9
10 674 Loeb, L.A., Preston, B.D., Snow, E.T., and Schaaper, R.M. (1986) Apurinic sites as common
11
12 675 intermediates in mutagenesis. *Basic Life Sci* **38**: 341-347.
13
14
15 676 McCulloch, S.D., and Kunkel, T.A. (2006) Multiple solutions to inefficient lesion bypass by T7
16
17 677 DNA polymerase. *DNA Repair (Amst)* **5**: 1373-1383.
18
19
20 678 McGlynn, P., and Lloyd, R.G. (2002) Recombinational repair and restart of damaged replication
21
22 679 forks. *Nat Rev Mol Cell Biol* **3**: 859-870.
23
24
25 680 Myllykallio, H., Lopez, P., Lopez Garcia, P., Heilig, R., Saurin, W., Zivanovic, Y., Philippe, H.,
26
27 681 and Forterre, P. (2000) Bacterial mode of replication with eukaryotic-like machinery in a
28
29 682 hyperthermophilic archaeon. *Science* **288**: 2212-2215.
30
31
32 683 Nohmi, T. (2006) Environmental Stress and Lesion-Bypass DNA Polymerases. *Annu Rev*
33
34 684 *Microbiol.*
35
36 685 Pages, V., and Fuchs, R.P. (2002) How DNA lesions are turned into mutations within cells?
37
38 686 *Oncogene* **21**: 8957-8966.
39
40
41 687 Pages, V., Janel-Bintz, R., and Fuchs, R.P. (2005) Pol III proofreading activity prevents lesion
42
43 688 bypass as evidenced by its molecular signature within E.coli cells. *J Mol Biol* **352**: 501-
44
45 689 509.
46
47
48 690 Park, D. (2007) Genomic DNA isolation from different biological materials. *Methods Mol Biol*
49
50 691 **353**: 3-13.
51
52
53 692 Rothwell, P.J., and Waksman, G. (2005) Structure and mechanism of DNA polymerases. *Adv*
54
55 693 *Protein Chem* **71**: 401-440.
56
57
58
59
60

- 1
2
3 694 Rouillon, C., Henneke, G., Flament, D., Querellou, J., and Raffin, J.P. (2007) DNA Polymerase
4
5 695 Switching on Homotrimeric PCNA at the Replication Fork of the Euryarchaea
6
7
8 696 *Pyrococcus abyssi*. *J Mol Biol* **369**: 343-355.
9
10 697 Schaaper, R.M., and Loeb, L.A. (1981) Depurination causes mutations in SOS-induced cells.
11
12 698 *Proc Natl Acad Sci U S A* **78**: 1773-1777.
13
14
15 699 Schaaper, R.M., Kunkel, T.A., and Loeb, L.A. (1983) Infidelity of DNA synthesis associated
16
17 700 with bypass of apurinic sites. *Proc Natl Acad Sci U S A* **80**: 487-491.
18
19
20 701 Scharer, O.D., and Jiricny, J. (2001) Recent progress in the biology, chemistry and structural
21
22 702 biology of DNA glycosylases. *Bioessays* **23**: 270-281.
23
24
25 703 Shibutani, S., Takeshita, M., and Grollman, A.P. (1997) Translesional synthesis on DNA
26
27 704 templates containing a single abasic site. A mechanistic study of the "A rule". *J Biol*
28
29 705 *Chem* **272**: 13916-13922.
30
31
32 706 Shimizu, K., Hashimoto, K., Kirchner, J.M., Nakai, W., Nishikawa, H., Resnick, M.A., and
33
34 707 Sugino, A. (2002) Fidelity of DNA polymerase epsilon holoenzyme from budding yeast
35
36 708 *Saccharomyces cerevisiae*. *J Biol Chem* **277**: 37422-37429.
37
38
39 709 Shimizu, M., Gruz, P., Kamiya, H., Kim, S.R., Pisani, F.M., Masutani, C., Kanke, Y.,
40
41 710 Harashima, H., Hanaoka, F., and Nohmi, T. (2003) Erroneous incorporation of oxidized
42
43 711 DNA precursors by Y-family DNA polymerases. *EMBO Rep* **4**: 269-273.
44
45
46 712 Strauss, B.S. (1991) The 'A rule' of mutagen specificity: a consequence of DNA polymerase
47
48 713 bypass of non-instructional lesions? *Bioessays* **13**: 79-84.
49
50
51 714 Tanguy Le Gac, N., Delagoutte, E., Germain, M., and Villani, G. (2004) Inactivation of the 3'-5'
52
53 715 exonuclease of the replicative T4 DNA polymerase allows translesion DNA synthesis at
54
55 716 an abasic site. *J Mol Biol* **336**: 1023-1034.
56
57
58
59
60

- 1
2
3 717 Taylor, J.S. (2002) New structural and mechanistic insight into the A-rule and the instructional
4
5 718 and non-instructional behavior of DNA photoproducts and other lesions. *Mutat Res* **510**:
6
7 719 55-70.
8
9
10 720 Villani, G., Boiteux, S., and Radman, M. (1978) Mechanism of ultraviolet-induced mutagenesis:
11
12 721 extent and fidelity of in vitro DNA synthesis on irradiated templates. *Proc Natl Acad Sci*
13
14 722 *U S A* **75**: 3037-3041.
15
16
17 723 Yang, W. (2005) Portraits of a Y-family DNA polymerase. *FEBS Lett* **579**: 868-872.
18
19
20 724 Yang, W., and Woodgate, R. (2007) What a difference a decade makes: insights into translesion
21
22 725 DNA synthesis. *Proc Natl Acad Sci U S A* **104**: 15591-15598.
23
24
25 726 Zahn, K.E., Belrhali, H., Wallace, S.S., and Doublet, S. (2007) Caught bending the A-rule:
26
27 727 crystal structures of translesion DNA synthesis with a non-natural nucleotide.
28
29 728 *Biochemistry* **46**: 10551-10561.
30
31
32 729 Zhao, B., Xie, Z., Shen, H., and Wang, Z. (2004) Role of DNA polymerase eta in the bypass of
33
34 730 abasic sites in yeast cells. *Nucleic Acids Res* **32**: 3984-3994.
35
36
37 731 Zhao, H., Shen, J., Deininger, P., and Hunt, J.D. (2006) Abasic sites and survival in resected
38
39 732 patients with non-small cell lung cancer. *Cancer Lett.*
40
41 733
42
43
44 734
45
46
47
48
49
50
51
52
53
54
55
56
57
58
59
60

1
2
3 735 **FIGURE LEGENDS**
4

5 736 **Table 1. Damaged or intact oligonucleotides used in this study.** X represents the position of
6
7
8 737 the correct base, template C, or a tetrahydrofuran moiety designed to functionally mimic an
9
10 738 abasic site.
11

12
13 739

14
15 740 **Table 2. Incorporation kinetics by wild-type and exonuclease-deficient *Pabpols*.** Single
16
17 741 nucleotide insertion assays were performed as described in Experimental procedures. The
18
19 742 observed rates of deoxynucleotide incorporation as a function of dNTP concentration were firstly
20
21 743 determined from Lineweaver-Burk plots. The data were fit by nonlinear regression using the
22
23 744 Marquardt-Levenberg algorithm (EnzFitter 2.0, BioSoft) to the Michaelis-Menten equation
24
25 745 describing a hyperbola, $v = (V_{max} \times [dNTP]/K_m + [dNTP])$ as already described (Le Breton *et*
26
27 746 *al.*, 2007). Apparent K_m and V_{max} kinetic parameters were obtained from the fit and were used
28
29 747 to calculate the efficiency of deoxynucleotide incorporation (k_{cat}/K_m). The kinetics values are the
30
31 748 average of at least triplicate determinations and are shown with SD. The f (misinsertion
32
33 749 frequency) is the ratio k_{cat}/K_m for the incorrect nucleotide to k_{cat}/K_m for the correct nucleotide. ND
34
35 750 means no detectable incorporation observed.
36
37
38
39
40

41 751

42
43 752 **Figure 1. Rate of endogenous AP sites into *P. abyssi* and *E.coli* genomes at different growth**
44
45 753 **stages.** Steady-state level of AP sites per 100,000 bp was calculated during the exponential and
46
47 754 stationary phases of growth. The number of AP sites per 100,000 bp represents the mean of
48
49 755 triplicate experiments and error bars show the standard deviations of each measurement.
50

51 756
52
53
54
55
56
57
58
59
60

1
2
3 757 **Figure 2. Replication of AP sites containing M13mp18 DNA template by *Pabpols*. A,**
4
5
6 758 Chemical treatment to induced AP sites into M13mp18 DNA. **B,** Primer extension assays were
7
8 759 performed with 5'-fluorescein end labelled primer (oligonucleotide 6) hybridised to either the
9
10 760 damaged or undamaged M13mp18 DNA template, *Pabpols* and T4 DNA polymerase used as a
11
12 761 control experiment. The elongated products were separated on a 0.8 % (w/v) denaturing alkaline
13
14
15 762 agarose gel. Lanes 1, 2, 4, 6, 7, 9, 11, 12 are the undamaged extended products; lanes 3, 5, 8, 10,
16
17 763 13 are the damaged extended products. **C,** dNTPs incorporation into the damaged and
18
19
20 764 undamaged M13mp18 DNA primed-templates were tested by acid precipitation and incubation
21
22 765 was performed according to the dependent polymerase reactions with [³H]dTTP as the substrate
23
24 766 (as outlined in Experimental procedures).
25
26
27 767

Peer Review

28
29
30
31
32
33
34
35
36
37
38
39
40
41
42
43
44
45
46
47
48
49
50
51
52
53
54
55
56
57
58
59
60

1
2
3 768 **Figure 3. Replication of AP-containing mini-circular and linear oligonucleotides DNA**
4
5 769 **templates by the wild-type or exonuclease-deficient *PabpolB*.** Primer extension assays were
6
7
8 770 performed at the indicated *PabpolB* concentrations with 8.3 nM of primer-template
9
10 771 (oligonucleotides 1 and 5), 200 μ M dNTPs at 55°C for 30 min as described in the Experimental
11
12 772 procedures. Quantifications of the extended products from the AP site are mentioned below the
13
14
15 773 gels. The extent of the bypass reaction was calculated as the ratio of the intensity of the bands
16
17 774 downstream of the AP site to the intensity of the bands opposite the lesion. **A,** Replication onto
18
19 775 the AP site-containing linear template. The position of the abasic site is indicated by X. Lanes 2
20
21 776 and 9 correspond to the positive control with 8.3 nM of intact template (X=C). **B,** Replication of
22
23 777 the AP site-containing circular template. Lanes 2 and 8 correspond to the positive control with
24
25 778 8.3 nM of intact template (X=C). 32 mer indicates the position of the base preceding the AP site,
26
27 779 while 33 mer is the position of the AP site.
28
29
30
31
32
33

34 781 **Figure 4. Replication of AP-containing mini-circular and linear oligonucleotides DNA**
35
36 782 **templates by the wild-type or exonuclease-deficient *PabpolD*.** Primer extension assays were
37
38 783 performed at the indicated *PabpolD* concentrations with 8.3 nM of primer-template
39
40 784 (oligonucleotides 1 and 5), 200 μ M dNTPs at 55°C for 30 min as described in the Experimental
41
42 785 procedures. Quantification of the extended products from the AP site is mentioned below the
43
44 786 gels. The extent of the bypass reaction was calculated as the ratio of the intensity of the bands
45
46 787 downstream of the AP site to the intensity of the bands opposite the lesion. **A,** Replication onto
47
48 788 the AP site-containing linear template. The position of the abasic site is indicated by X. Lanes 2
49
50 789 and 8 correspond to the positive control with 8.3 nM of template (X=C). **B,** Replication of the
51
52 790 AP site-containing circular template. Lanes 2 and 8 correspond to the positive control with 8.3
53
54
55
56
57
58
59
60

1
2
3 791 nM of template (X=C). 32 mer indicates the position of the base preceding the AP site, while 33
4
5 792 mer is the position of the AP site.
6
7

8 793

9
10 794 **Figure 5. Effect of varying the downstream template base on nucleotide incorporation**

11 **opposite an AP site by *Pabpol*s.** Standing start reactions were performed with four DNA

12 795 templates that varied by the nature of the 5' template base. The fluorescein-labelled primer

13 796 (oligonucleotide 6) was annealed right before the template AP site that is indicated by X.

14 797 Different template bases 5' to the AP site are depicted by N (N=A, oligonucleotide 2; N=T,

15 798 oligonucleotide 1; N=G, oligonucleotide 3; N=C, oligonucleotide 4) (Table 1). Single nucleotide

16 800 incorporations were carried out as described in Experimental procedures with the different

17 801 primed-templates, 13 nM of *PabpolB* *exo*⁺/*exo*⁻, 20 nM of *PabpolD* *exo*⁺/*exo*⁻, 200 μM of each

18 802 dNTP at 55°C for 30 min. A. Reaction with 13 nM *PabpolB* *exo*⁺. B. Reaction with 20 nM

19 803 *PabpolD* *exo*⁺. C. Reaction with 13 nM *PabpolB* *exo*⁻. D. Reaction with 20 nM *PabpolD* *exo*⁺.

20
21
22
23
24
25
26
27
28
29
30
31
32
33
34
35
36
37
38
39
40
41
42
43
44
45
46
47
48
49
50
51
52
53
54
55
56
57
58
59
60

804

Oligonucleotide 15' -CAGGAAACAGCTATGACCATGATTACGAATTCGAGCTCGGTACCCGGGGATCC**T**XTAGAGTCGACCTGCAGGCATGCAAGCTTGGCA-3'**Oligonucleotide 2**5' -CAGGAAACAGCTATGACCATGATTACGAATTCGAGCTCGGTACCCGGGGATCC**A**XTAGAGTCGACCTGCAGGCATGCAAGCTTGGCA-3'**Oligonucleotide 3**5' -CAGGAAACAGCTATGACCATGATTACGAATTCGAGCTCGGTACCCGGGGATCC**G**XTAGAGTCGACCTGCAGGCATGCAAGCTTGGCA-3'**Oligonucleotide 4**5' -CAGGAAACAGCTATGACCATGATTACGAATTCGAGCTCGGTACCCGGGGATCC**C**XTAGAGTCGACCTGCAGGCATGCAAGCTTGGCA-3'**Oligonucleotide 5**

5' -TGCCAAGCTTGCATGCC-3'

Oligonucleotide 6

5' -TGCCAAGCTTGCATGCCTGCAGGTCGACTCTA-3'

805

806 **Table 1 : Damaged or intact oligonucleotides used in this study**

For Peer Review

807

DNA polymerase	dNTP	K_m (μM)	k_{cat} (min^{-1})	k_{cat}/K_m ($\mu\text{M}^{-1} \text{min}^{-1}$)	$f(\text{misinsertion frequency})$	
Insertion opposite C	<i>PabpolB</i> exo+	dATP	ND	ND	ND	
		dTTP	ND	ND	ND	
		dGTP	0.25±0.01	425.27 ±0.12	1671.5	
		dCTP	ND	ND	ND	
	<i>PabpolD</i> exo+	dATP	ND	ND	ND	
		dTTP	ND	ND	ND	
		dGTP	0.19±0.02	66.70±0.69	346.36	
		dCTP	ND	ND	ND	
	<i>PabpolB</i> exo-	dATP	18.70±1.23	61.09±0.43	3.27	0.11
		dTTP	5.46±0.05	35.05±0.86	6.42	0.21
		dGTP	1.98±0.35	60.29±0.15	30.41	1.00
		dCTP	32.01±2.11	23.07±0.37	0.72	0.02
<i>PabpolD</i> exo-		dATP	74.47±9.16	39.71±1.28	0.53	0.16
		dTTP	17.00±3.50	32.50±1.30	1.91	0.57
		dGTP	13.93±1.08	46.81±8.60	3.36	1.00
		dCTP	374.69±129.32	10.41±8.20	0.03	0.01
Insertion opposite AP site	<i>PabpolB</i> exo+	dATP	100±9	87±4	0.79	
		dTTP	121±7	91±4	0.75	
		dGTP	610±40	120±8	0.20	
		dCTP	ND	ND	ND	
	<i>PabpolD</i> exo+	dATP	36±3	114±4	3.17	
		dTTP	650±20	102±2	0.16	
		dGTP	ND	ND	ND	
		dCTP	ND	ND	ND	
	<i>PabpolB</i> exo-	dATP	4.19±0.31	89.42±1.23	21.35	
		dTTP	15.02±0.18	62.92±0.11	4.19	
		dGTP	8.88±2.35	73.68±4.71	8.30	
		dCTP	ND	ND	ND	
		<i>PabpolD</i> exo-	dATP	12.00±2.41	29.03±1.32	2.42
			dTTP	76.19±0.85	25.55±0.07	0.34
			dGTP	70.41±7.61	12.43±0.36	0.18
			dCTP	82.08±6.12	30.72±0.54	0.37

808

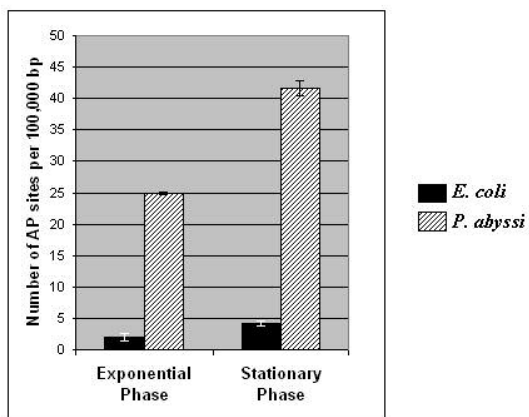
809

810 **Table 2 : Incorporation kinetics by wild-type and exonuclease-deficient *Pabpols***

811

812

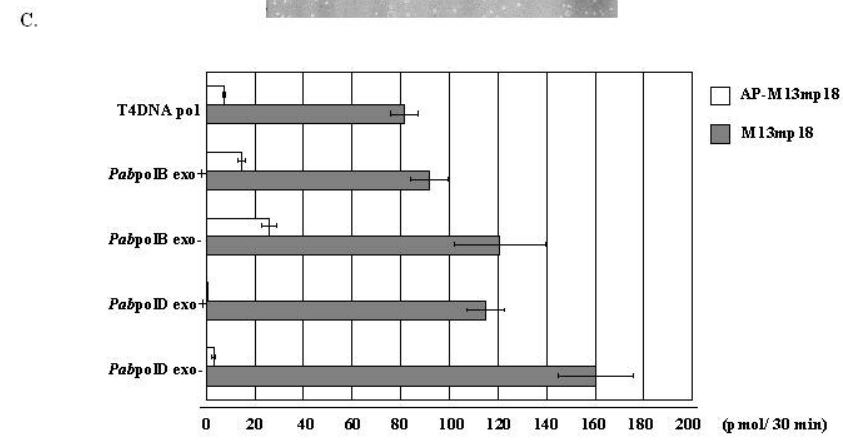
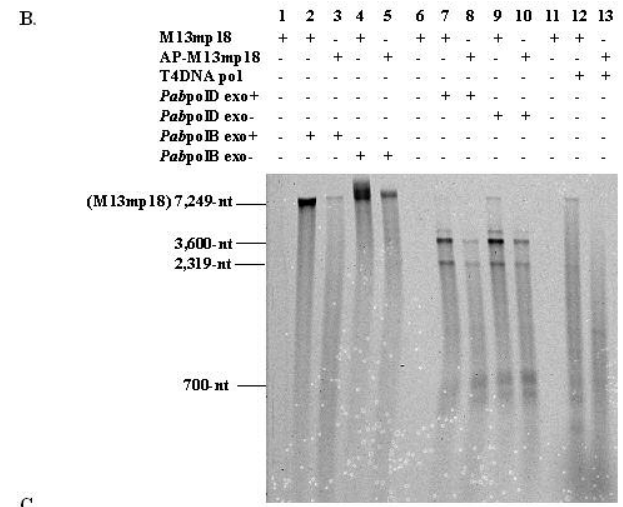
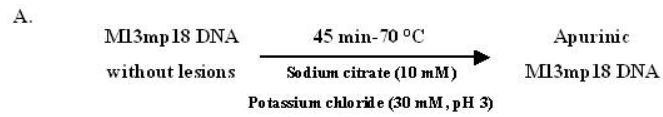
1
2
3
4
5
6
7
8
9
10
11
12
13
14
15
16
17
18
19
20
21
22
23
24
25
26
27
28
29
30
31
32
33
34
35
36
37
38
39
40
41
42
43
44
45
46
47
48
49
50
51
52
53
54
55
56
57
58
59
60



190x254mm (96 x 96 DPI)

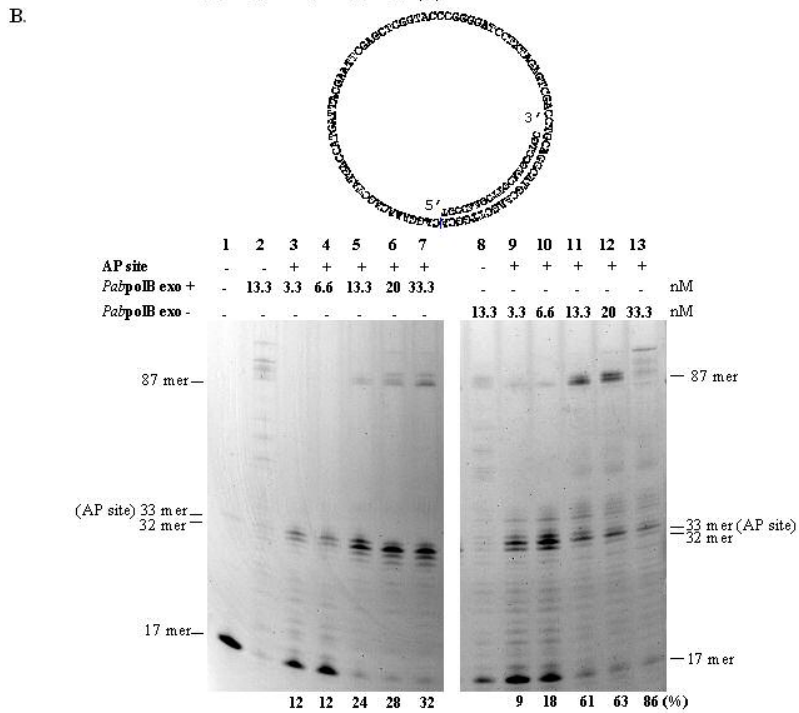
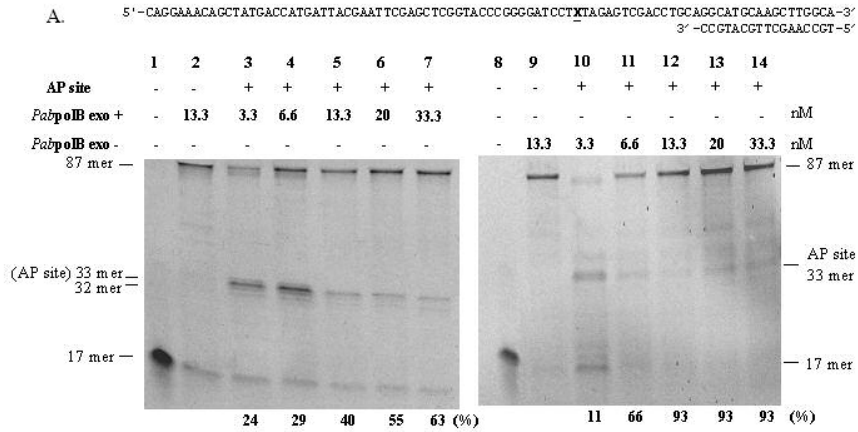
1
2
3
4
5
6
7
8
9
10
11
12
13
14
15
16
17
18
19
20
21
22
23
24
25
26
27
28
29
30
31
32
33
34
35
36
37
38
39
40
41
42
43
44
45
46
47
48
49
50
51
52
53
54
55
56
57
58
59
60

1
2
3
4
5
6
7
8
9
10
11
12
13
14
15
16
17
18
19
20
21
22
23
24
25
26
27
28
29
30
31
32
33
34
35
36
37
38
39
40
41
42
43
44
45
46
47
48
49
50
51
52
53
54
55
56
57
58
59
60



190x254mm (96 x 96 DPI)

1
2
3
4
5
6
7
8
9
10
11
12
13
14
15
16
17
18
19
20
21
22
23
24
25
26
27
28
29
30
31
32
33
34
35
36
37
38
39
40
41
42
43
44
45
46
47
48
49
50
51
52
53
54
55
56
57
58
59
60



190x254mm (96 x 96 DPI)

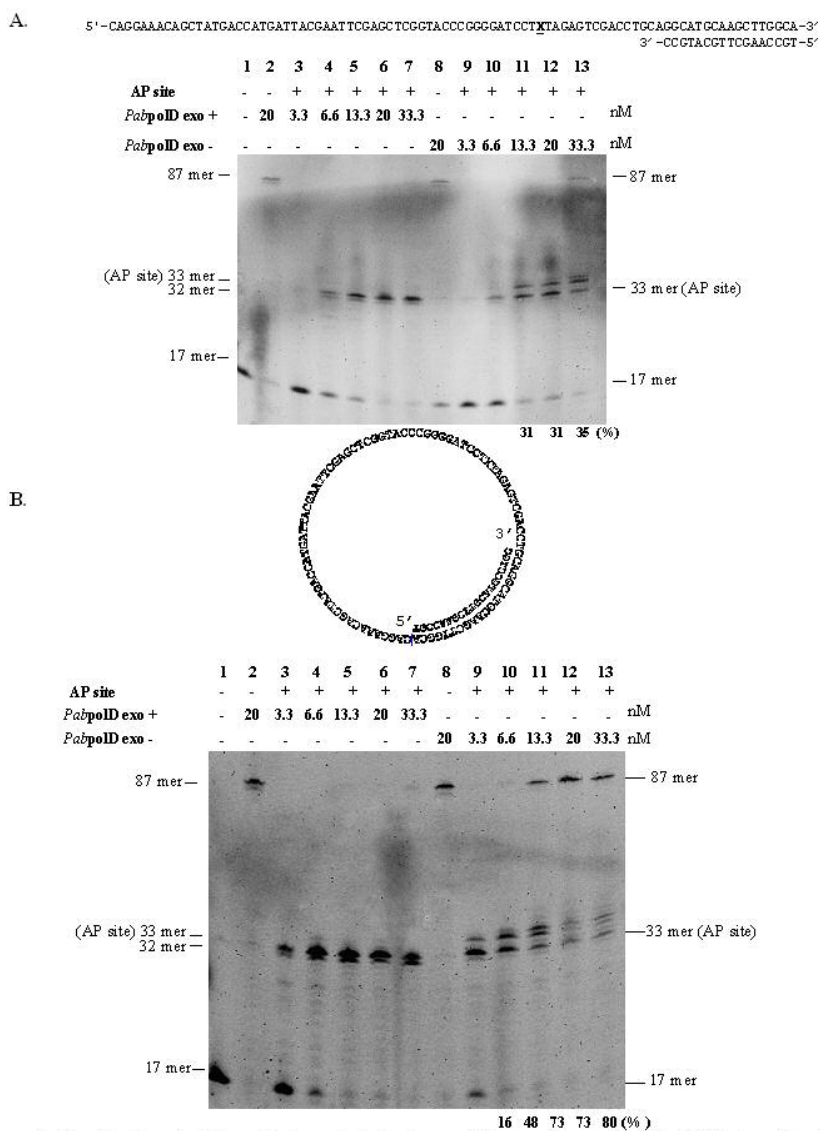
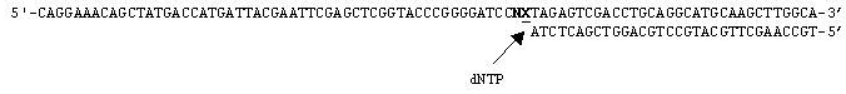
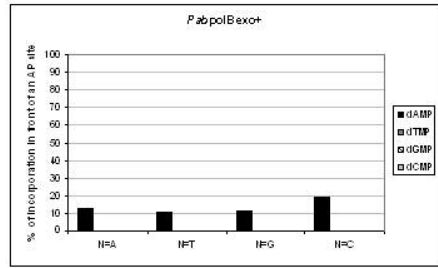


Figure 4 : Replication of AP-containing mini-circular and linear oligonucleotides DNA templates by the wild-type or exonuclease-deficient *Pabp1D*

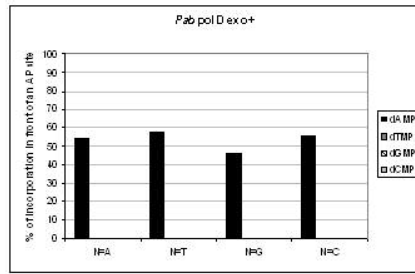
190x254mm (96 x 96 DPI)



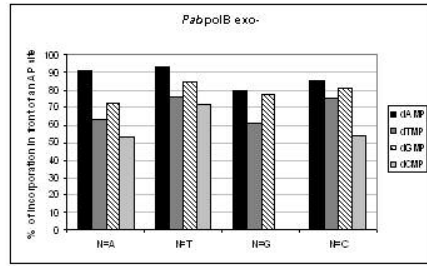
A.



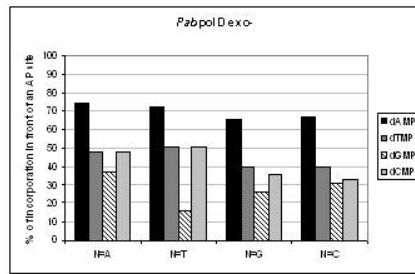
B.



C.



D.



190x254mm (96 x 96 DPI)

1
2
3
4
5
6
7
8
9
10
11
12
13
14
15
16
17
18
19
20
21
22
23
24
25
26
27
28
29
30
31
32
33
34
35
36
37
38
39
40
41
42
43
44
45
46
47
48
49
50
51
52
53
54
55
56
57
58
59
60